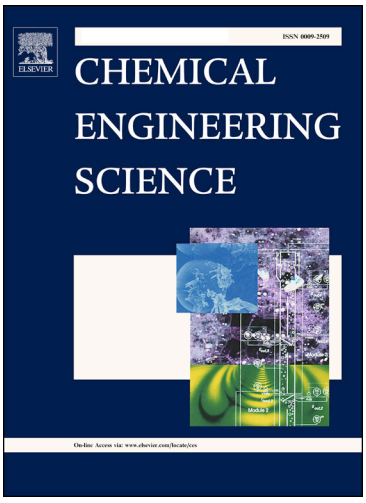

Effects of Temperature on Methanol Adsorption on Functionalized Graphite: Saturation of Functional Groups

Waralee Dilokekunakul, Nikom Klomkliang, Somsak Supasitmongkol, Somboon Chaemchuen, D.D. Do, D. Nicholson

PII: S0009-2509(18)30277-X
DOI: https://doi.org/10.1016/j.ces.2018.04.063
Reference: CES 14195

To appear in: *Chemical Engineering Science*

Received Date: 20 February 2018
Revised Date: 19 April 2018
Accepted Date: 27 April 2018

Please cite this article as: W. Dilokekunakul, N. Klomkliang, S. Supasitmongkol, S. Chaemchuen, D.D. Do, D. Nicholson, Effects of Temperature on Methanol Adsorption on Functionalized Graphite: Saturation of Functional Groups, *Chemical Engineering Science* (2018), doi: https://doi.org/10.1016/j.ces.2018.04.063

Effects of Temperature on Methanol Adsorption on Functionalized Graphite: Saturation of Functional Groups

by

Waralee Dilokekunakul [a], Nikom Klomkliang [b,*], Somsak Supasitmongkol [c], Somboon Chaemchuen [d], D. D. Do [e], and D. Nicholson [e]

[a] Department of Chemical Engineering, Mahidol University, Nakhon Pathom 73170, Thailand
[b] School of Chemical Engineering, Suranaree University of Technology, Nakhon Ratchasima 30000, Thailand
[c] National Metal and Materials Technology Center, Pathumtani 12120, Thailand
[d] State Key Laboratory of Advanced Technology for Materials Synthesis and Processing; Center for Chemical and Material Engineering, Wuhan University of Technology, Wuhan 430070, P.R. China
[e] School of Chemical Engineering, University of Queensland, St. Lucia, QLD 4072, Australia

Abstract

Grand Canonical Monte Carlo simulation of methanol adsorption on a graphite model with two hydroxyl groups grafted on the surface has been carried out to investigate the effects of temperature in the range of 278-360K. The spacing between the OH groups was chosen so that two hydrogen bonds could be formed with the first methanol molecule. In the Henry law region, the isosteric heat at zero loading is greater than the condensation heat. When the loading is increased, the isosteric heat at low temperatures decreases slightly and exhibits a shoulder, which is associated with the formation of a cluster of methanol molecules around one OH group. On further increase in loading, the adsorbate-adsorbate interactions decrease because methanol begins to adsorb on the other OH group, resulting in a sharp decrease in the isosteric heat to a minimum, at which point both OH groups are covered with methanol molecules. At higher temperatures the isosteric heat at zero loading decreases but remains higher than the condensation heat. The shoulder heat is progressively diminished with temperature because methanol molecules are distributed over the two OH groups, due to the entropic effects. Interestingly, the minimum heat still occurs when the functional groups are covered and is even more pronounced at high temperatures.

Keywords: Methanol adsorption; Carbon; Isosteric heat; Functional group; Molecular simulation

*Corresponding authors: nikom.klo@sut.ac.th

1. Introduction

Physical adsorption of non-polar gases is commonly used to characterize the physical properties of porous materials (Joyner, 1948; Haul, 1982; Gregg, 1982; Roberts et al., 1987; Yin et al., 1999; Thommes, 2005; Morishige, 2006; Rasmussen, 2010; Fan et al., 2011; Reichenbach et al., 2011; Nguyen et al., 2013; Klomkliang et al., 2014, 2015; Alabadi et al., 2015; Zelenka, 2016; Cychosz et al., 2017) because of the absence of electrostatic interactions. Attention has also been paid to the use of polar fluids, such as water and methanol, for the characterization of surface chemistry because of their stronger interactions with functional groups than with the basal plane of carbon (Morimoto and Miura, 1985, 1991; Sing, 1985; Bandosz et al., 1996; Easton and Machin, 2000; Ohba and Kaneko, 2007; Wongkoblap and Do, 2007; Nguyen et al., 2011; Nguyen et al., 2013; Factorovich et al., 2014; Kaneko, 2015; Zeng et al., 2015; Klomkliang et al., 2016; Kowalczyk et al., 2017; Sarkisov et al., 2017).

Early experiments on the adsorption of water and methanol on carbonaceous materials were made by Pierce and Smith in 1950. Since then there have been many reports in the literature highlighting the important role of polar fluids in characterizing surface chemistry; for example (Morimoto and Miura, 1985, 1986, 1991; Zeng et al., 2015; and Salame and Bandosz, 1999, 2000). An interesting observation in the adsorption of methanol on graphitized carbon black is the existence of a minimum in the plot of the isosteric heat at the loading where the functional groups are covered with adsorbate molecules (Klomkliang et al., 2016). When the pressure is increased beyond this point, methanol spills over onto the basal plane at sub-monolayer coverage, because there is a strong dispersion force interaction between the methyl group and the basal plane. Beyond this multilayers are formed. However, the part that the configuration of functional groups plays in this phenomenon, has not been elaborated. Recently, Klomkliang et al., 2017 studied the effects on methanol adsorption, of the orientation and separation of two hydroxyl groups mounted on a graphite surface, and showed that orientation modifies the isosteric heat curve over the range of loadings where the functional groups are progressively covered with methanol molecules. The isosteric heat curves were classified into two groups depending on whether the initial isosteric heat was greater or less than the condensation heat. When the two hydroxyl groups are separated by

0.5nm and their respective hydrogen atoms point towards each other, the isosteric heat at zero loading is highest. This is because two hydrogen bonds can be formed between one methanol molecule and the two hydroxyl groups. When the functional groups are covered, the isosteric heat decreases to a minimum, and we shall refer to this as the saturation of the functional groups.

The behaviour of the isosteric heat versus loading is a result of the interplay of two interactions between methanol and the adsorbent: (1) an electrostatic interaction with the functional groups and (2) a vdW interaction with the graphite. The latter becomes more significant as temperature increases, because of the large area of the graphite surface (entropic effects). In this paper we extend the previous work of Klomkliang et al., 2017 to investigate the microscopic origin of the effects of temperature on the minimum heat.

2. Theory and method

2.1 Fluid-Fluid potential energy

The intermolecular interaction energy between the two adsorbate molecules is calculated as the sum of the pairwise dispersive, electrostatic and repulsive potential energies (Klomkliang et al., 2017). Many potential models for methanol have been proposed in the literature; here we chose the TraPPE-UA model (Chen et al., 2001) because it gives a good description of the vapor-liquid equilibrium, which has been found as the prerequisite to correctly describe adsorption. Its molecular parameters are shown in Table 1.

Table 1 Molecular parameters of methanol using TraPPE-UA model and hydroxyl group.

Fluid/ Functional group	x (nm)	y (nm)	z (nm)	ε/k_B (K)	σ (nm)	q (e)
Methanol						
CH_3	0.14300	0	0	98.0	0.375	+0.265
O	0	0	0	93.0	0.302	-0.700
H	-0.02998	0.08961	0	-	-	+0.435
Hydroxyl group						
O	0	0	0.13640	78.2	0.307	-0.64
H	0	0.08992	0.17002	-	-	+0.44

C (Graphene)	0	0	0	-	-	+0.20

2.2 Fluid-Solid potential energy

The interaction between an adsorbate molecule and the graphite surface was calculated by the 10-4-3 potential equation (Steele, 1973) for a homogeneous surface, using an atomic surface density of 38.2nm^{-2}, and a spacing between graphene layers of 0.3354nm. The molecular parameters for a carbon atom in the adsorbent are $\sigma_i^{(S)}$= 0.34nm and $\varepsilon_i^{(S)}/k_B$= 28K.

2.3 Surface functional group potential model

There is no doubt that the surface chemistry of real materials is very complex. Even when two samples are prepared from the same precursor under the same preparation conditions, the identity, concentration and configuration of functional groups may be different. Here we have used a simple model that captures the main physical features of real materials. Hydroxyl groups were chosen as the functional group, because they are found in many carbon materials after heat treatment (Morimoto and Miura, 1985, 1986; Miura and Morimoto, 1991; Klomkliang et al., 2017) and were grafted onto a graphite surface.

We mounted two hydroxyl groups on top of the graphite surface separated by 0.5nm with their respective hydrogen atoms pointing toward each other (Figure 1a). With this configuration, two hydrogen bonds can form between one methanol molecule and the two OH groups which gives the maximum heat at zero loading (Klomkliang et al., 2016, 2017). The molecular parameters for the hydroxyl group model (Mooney et al., 1998) are listed in Table 1.

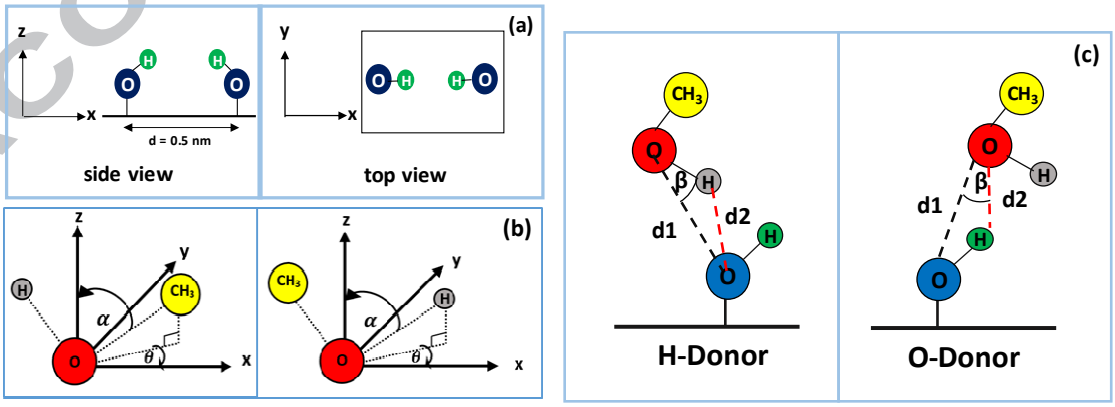

Figure 1 (**a**) Side and top views of two hydroxyl groups with the inward configuration on a graphene basal plane. (**b**) α is the angle formed between the vector along O-H or O-CH_3 with respect to the normal vector from the surface, and θ is the angle formed between the projection of the OH or O-CH_3 vector onto the xy plane and the x-axis. (c) the definition of an H-bond; taken from (Chen et al., 2001; Pagliai, 2003).

2.4 Grand Canonical Monte Carlo simulation

Grand Canonical Monte Carlo simulation was used to obtain adsorption isotherms and isosteric heats with 5×10^6 cycles in the equilibration and sampling stages. The standard Metropolis scheme (Allen, 1989) was adopted with 1,000 insertion, deletion and displacement moves with equal probability for each cycle. The x- and y-dimensions of the graphite surface are 6nm×6nm, the cut-off radius is 3nm and the graphitic surface is positioned at the bottom (z = 0) of the simulation box, and the opposite side in the z-direction is treated as a hard wall. The box height is 8nm.

The average surface excess density was calculated from the following equation:

$$\Gamma_{avg} = \frac{\langle N \rangle - \rho_b V_{acc}}{A} \quad (1)$$

where $\langle N \rangle$ refers to the average number of adsorbate particles, ρ_b is the bulk molecular density, V_{acc} is the accessible pore volume of the bulk phase (Do et al., 2008) and A is the surface area of graphite.

The isosteric heat was calculated from fluctuation theory (Nicholson and Parsonage, 1982)

$$q_{x\text{-}y} = \frac{\langle U_{x\text{-}y} \rangle \langle N \rangle - \langle U_{x\text{-}y} N \rangle}{\langle N^2 \rangle - \langle N \rangle \langle N \rangle} \quad (2)$$

where $U_{x,y}$ is the configuration energy of interaction between x and y entities. The isosteric heat is calculated as the sum of contributions from the following interactions: fluid-fluid (F-F), fluid-functional group (F-Fn), fluid-graphite basal plane (F-Gr), and the kinetic energy:

$$q_{iso} = q_{F\text{-}F} + q_{F\text{-}Fn} + q_{F\text{-}Gr} + k_B T \quad (3)$$

The local density of a site in a methanol molecule, normal to the surface, is determined by:

$$\rho(z) = \frac{\langle \Delta N_{z+\Delta z} \rangle}{L_x L_y \Delta z} \quad (4)$$

where $<\Delta N_{z+\Delta z}>$ is the average number at that site in the region bounded by z and $z+\Delta z$.

The system was also divided in the x and y directions to study the two-dimensional density as follows from:

$$\rho(x,y)=\frac{<N_{(\Delta x,\Delta y)}>}{\Delta x \Delta y L_z} \quad (5)$$

where $<N_{(\Delta x,\ \Delta y)}>$ is the average number of O-atom between the boundary $(x-\Delta x/2,\ x+\Delta x/2)$ and $(y-\Delta y/2,\ y+\Delta y/2)$ and L_z is the box length in the z direction.

The O-H and O-CH_3 vectors (see Figure 1b) were used to analyse the orientation of the methanol molecules.

3. Results and discussion

3.1 Adsorption isotherm

The simulated isotherms and the experimental data (Nguyen et al., 2011, 2013) for temperatures in the range of 278-360K are shown in Figure 2. The experimental data are more sensitive to temperature than the simulation results at low loadings because the simulation model is a very simplistic representation of a complex physical reality. Despite this, the simulation results agree qualitatively with experimental data.

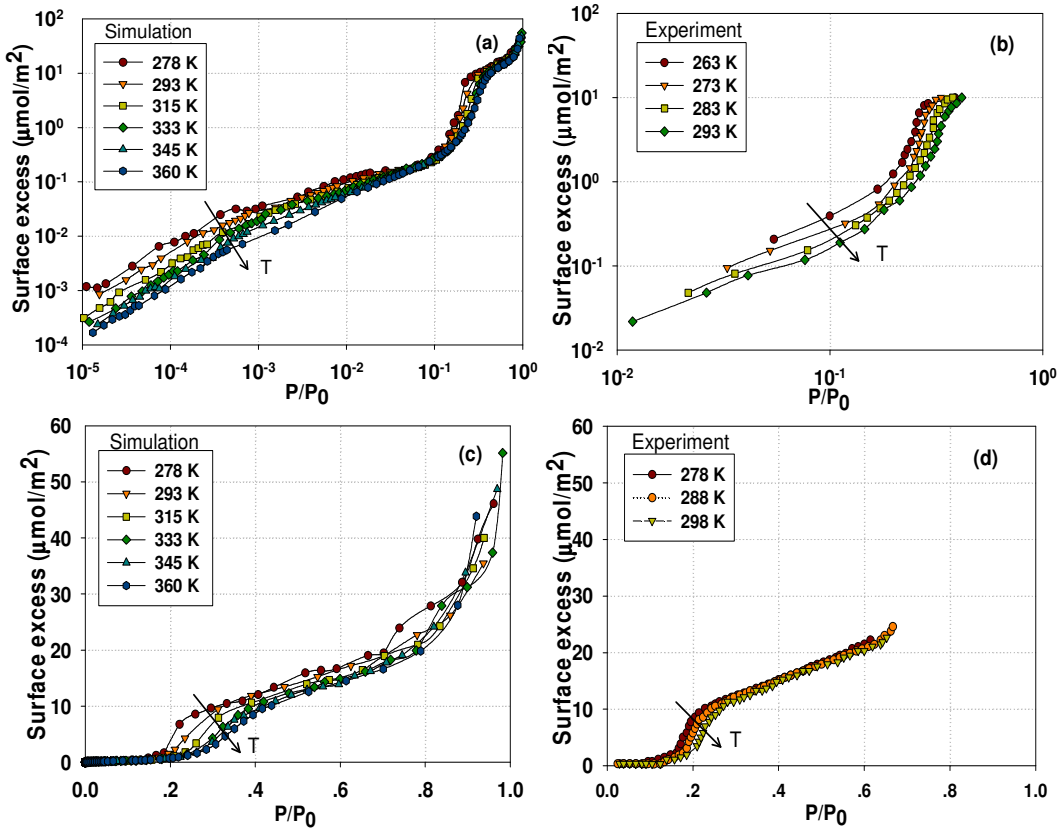

Figure 2. Adsorption of methanol on graphite at various temperatures: (a) simulated isotherms plotted on a logarithmic scale; (b) experimental isotherms on a logarithmic scale (Nguyen et al., 2013); (c) simulated isotherms on a linear scale, and (d) experimental isotherms on a linear scale (Nguyen et al., 2011). Vapor pressures of the methanol model were obtained from the literature (Nguyen et al., 2011).

3.2 Isosteric heat

The isosteric heats versus loading at various temperatures are shown in Figure 3a. The simulation results qualitatively describe the minimum in the experimental data of isosteric heat versus loading. Our simulation shows a minimum in the isosteric heat at a loading 0.26 µmole/m^2 when the functional groups are saturated with adsorbate. The experimental data (red line) display two minima at loadings of 0.1 and 0.5 µmole/m^2 (Klomkliang et al., 2017). The difference is attributed to the complexity of real materials.

Comparing the simulation results for the heats with or without a functional group, we see that the isosteric heat curves for these two cases merge at 0.26µmol/m^2, beyond which they

coincide. This indicates that at this loading the functional groups are covered with methanol molecules.

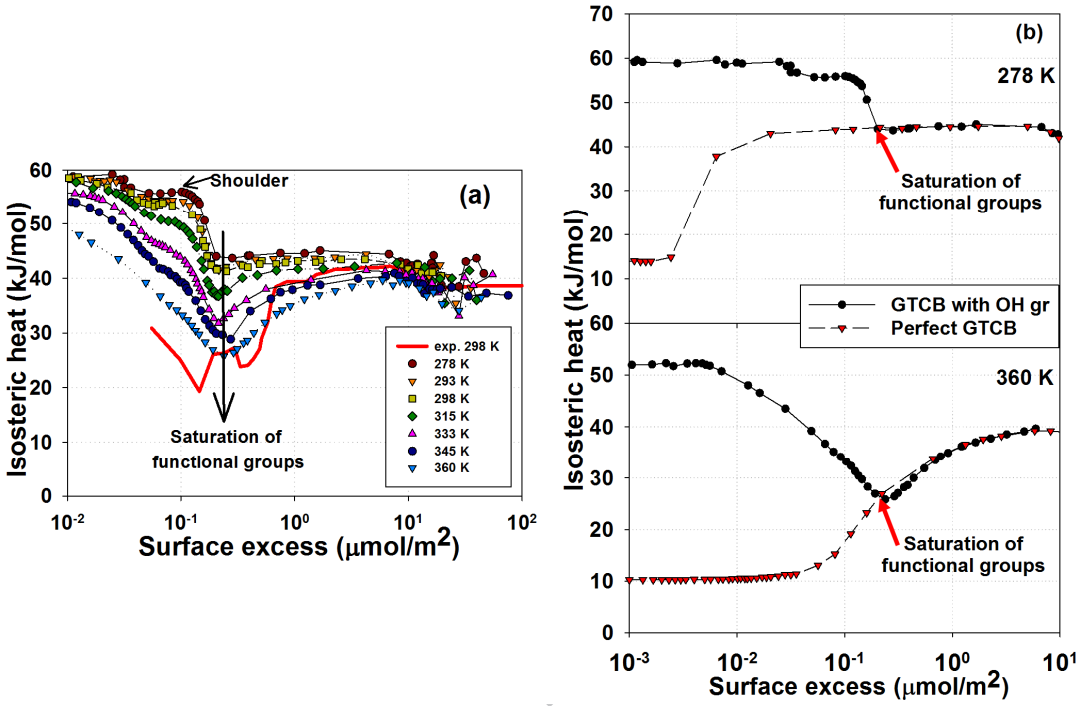

Figure 3. The total isosteric heats for methanol adsorbed on graphite: (a) simulation results at various temperatures from 278 to 360 K and experimental data at 298K (Klomkliang et al., 2017); (b) simulation for adsorption on pure GTCB in comparison with functionalized GTCB at 278 K (top) and 360 K (bottom)

The isosteric heat at zero loadings on the functionalized graphite is higher because of the additional electrostatic interaction between methanol and the functional groups. The heats for the functionalized surface are also distinguished by: (1) Oscillations at lower temperatures and (2) a more pronounced minimum at higher temperatures.

3.3 Contribution heats

The three contributions to the isosteric heat from functional group interactions, SF and FF interactions are shown in Figure 4 for temperatures between 278K and 360K. These graphs show that the minimum in the isosteric heat is coincided with the complete coverage of the functional groups as indicated by the decay of the F-Fn curve to zero.

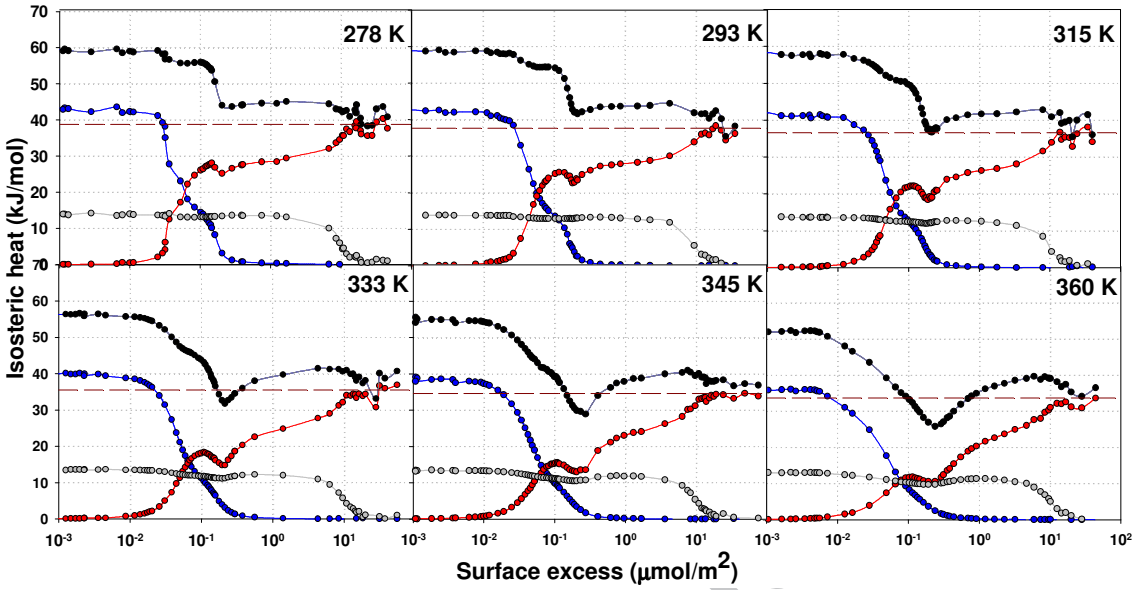

Figure 4. Contribution to the isosteric heats for methanol adsorption at various temperatures. The horizontal dashed line is the heat of condensation. The black symbols are the total heat, blue the F-Fn heat, gray the F-Gr heat, and red the F-F heat.

For loadings less than the threshold loading at the minimum, the contributions from the F-Fn and F-F interactions are greater for lower temperatures, resulting from the higher number of methanol molecules preferring one of the two OH groups. When the loading is increased the contribution from the F-F interactions decreases sharply because methanol begins to adsorb on the other functional group, and it reaches a minimum at 0.26μmol/m^2 for all temperatures, which is the loading at the minimum of the isosteric heat. It may be concluded that the minimum is due to the complete coverage of the two OH groups.

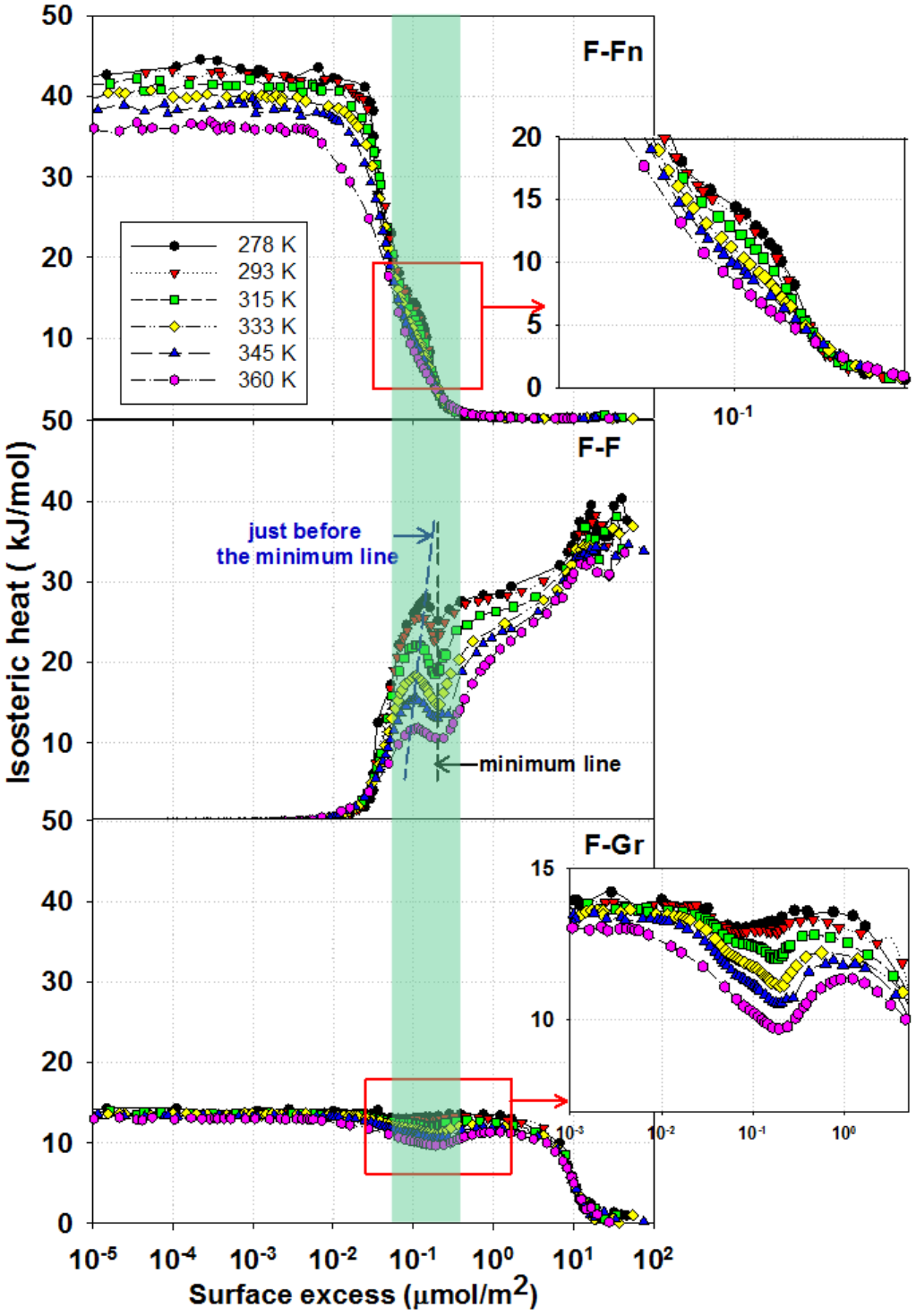

Figure 5. The comparison between isosteric heat from the fluid-functional group, (top), fluid-fluid (middle) and fluid-graphite (bottom) interactions at different temperatures. At the minimum line the functional groups are saturated.

The minimum heat is not only affected by the F-F and F-Fn contributions, but also by the contribution from the F-Gr interactions as shown in Figure 5. The contribution from the F-Gr interactions reaches a minimum when the functional groups are saturated and become more pronounced with temperature. This is explained by the change in the local density distribution of the CH_3 site with temperature as shown in Figure 6, which is more delocalised at 360K because of larger thermal fluctuations.

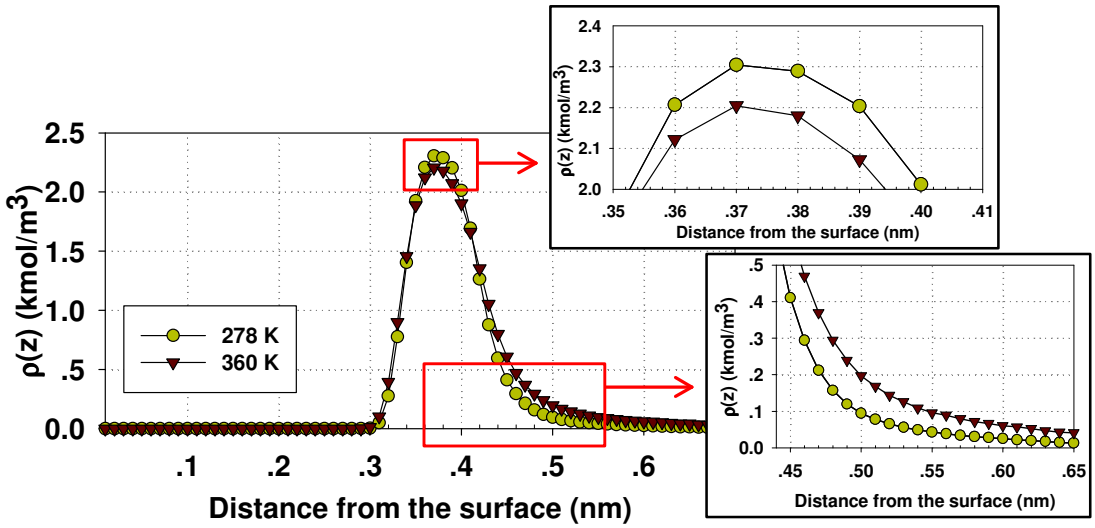

Figure 6. The local density distribution in the z direction of the CH_3 site at the saturation of the functional groups at 278 and 360K

Figure 7 shows the contributions to the heats at 278K and 360K as a function of loading, divided into Regions I-III, Point IV, and Regions V-VI. The corresponding local density distributions, angular distrubutions and snapshots are shown in Figures 8-10.

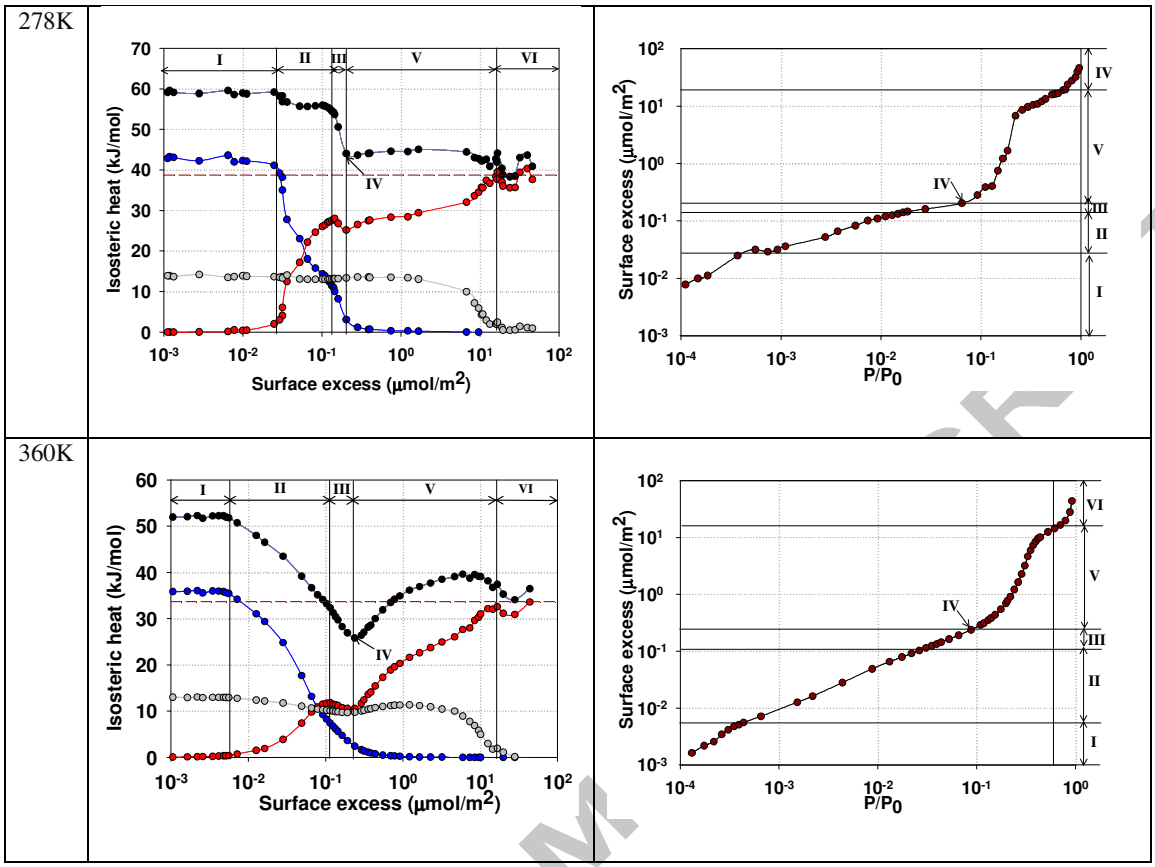

Figure 7. The isosteric heat versus loading and adsorption isotherm at 278 and 360K. The condensation heat is show as the horizontal dash line. The symbols in black show the total heat, blue the F-Fn heat, gray the F-Gr heat, and red the F-F heat. The adsorption process is divided into Regions I-III, Point IV, and Regions V-VI.

3.4 Microscopic behaviour at 278K and 360K

Region I (278K). In this Henry law region, the isosteric heat is constant at about 60kJ/mol, 44kJ/mol of which is contributed from the F-Fn interactions resulting from the formation of two hydrogen bonds between the O atom of the first methanol molecule and the two functional groups (see the 2D local density distribution in Figure 8). The remaining contribution to the isosteric heat is from the F-Gr interactions. The vectors along O-H and O-CH_3, show that molecules adopt angles less than 90^o, indicating that the H and CH_3 atoms are pointing away from the surface (Figure 8).

Region I (360K): At this temperature the trend is somewhat similar to that at 278K with the local angular distribution at 360K more diffuse, due to the greater thermal fluctuation.

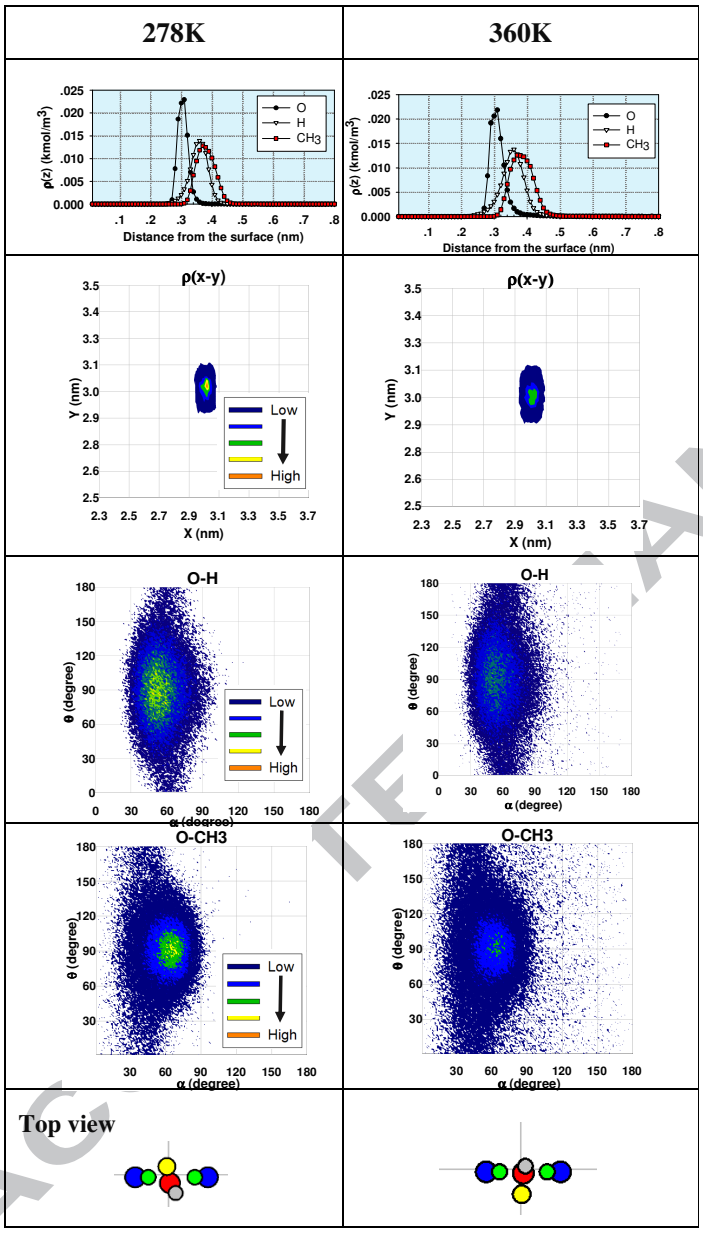

Figure 8. The local density distributions, angular distributions and snapshots (Top view) of Region I. O and H atoms of the functional groups are shown in blue and green, respectively. O and H atoms, and CH_3 site of methanol are represented in red, grey, and yellow, respectively.

Region II (278K): The isosteric heat decreases to 56kJ/mol and remains constant in this region, where there is a trade-off between the decrease in the contribution from the F-Fn interactions and the increase in the contribution from the F-F interactions. In this region a new methanol molecule interacts with one of the functional groups and with the first adsorbed molecule, which has to re-orient itself to accommodate new molecules until four molecules cover this functional group, called OH_1. One of the four methanol molecules form one hydrogen bond with the other side of OH_1 and another hydrogen bond with the neighbouring molecule. Therefore, there are three hydrogen bonds due to the F-Fn interactions and three hydrogen bonds due to the F-F interactions among these four molecules, resulting in a sharp decrease and an increase of the F-Fn and F-F interactions, respectively. The contribution from the F-Gr interactions remains constant because the methyl groups reside at the same distance from the graphite surface. The formation is summarised in Figure 9. The local density distribution of the H-atom of the methanol molecules in the z direction shows a minor peak at a closer distance to the surface than the major peak. The angular distributions of the vectors O-H and O-CH_3 of the main peak of the first adsorbed molecule) show similar configurations as those for Region I (where there is only one molecule). They also show the configurations of the additional molecules. These angles show that the H atom and CH_3 site of a newly adsorbed molecule can be either further away from the surface or nearer to the surface than the O atom.

Region II (360K): The shoulder disappears at 360K because the F-F contribution decreases due to larger thermal fluctuation and because there are only three methanol molecules on OH_1, compared to four at 278K (Figure 9).

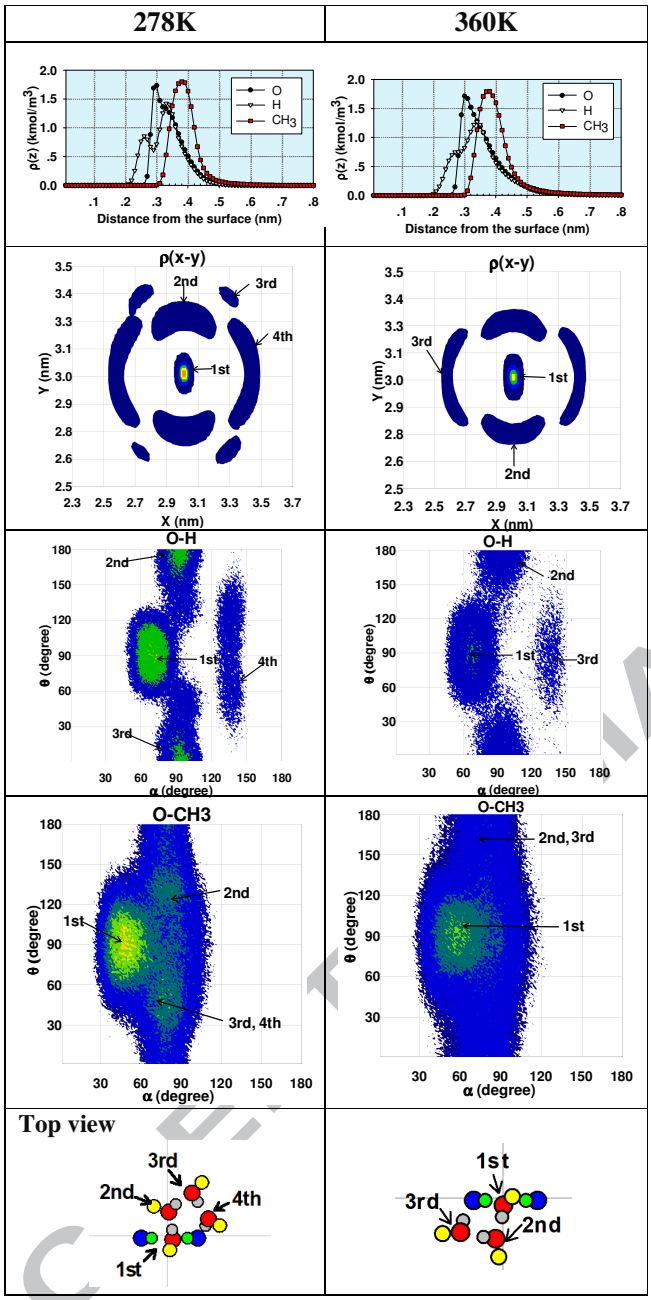

Figure 9. The local density distributions, angular distributions and snapshots at the last boundary of Region II.

Region III (278K): The isosteric heat decreases steeply because all contributions, from the F-F, F-Fn and F-Gr interactions decrease. The decrease of the F-F contribution is because the fifth

molecule forms a hydrogen bond with the other hydroxyl group, OH_2. The F-Fn interactions decrease because of the change in the hydrogen bond lengths and angle illustrated in Figure 11. This figure explains why the contribution of the F-Fn interaction to the isosteric heat decreases in Region III, even though, a fifth methanol molecule forms a hydrogen bond with the other OH group (OH_2). The figure shows that the hydrogen bond lengths and angle change from those in Regions I and II, and converge to a constant value for loadings above that of the saturation of the functional groups. The local properties at the last point in this region, **Point IV,** are shown in Figure 10. The angular distributions of the vectors O-H and O-CH_3 have a higher density than in Region II, but at the same locations.

Region III (360K): At **Point IV** all the OH groups are covered (loading of 0.26μmol/m^2) and there are five molecules distributed as 3:2 on these groups, as shown in Figure 10, compared to 4:1 for 278K. The more even distribution in 360K is due to entropic effects at the higher temperature. At this saturation point, the contributions from the F-F and F-Gr interactions reach a minimum and that from the F-Fn interactions decays towards zero.

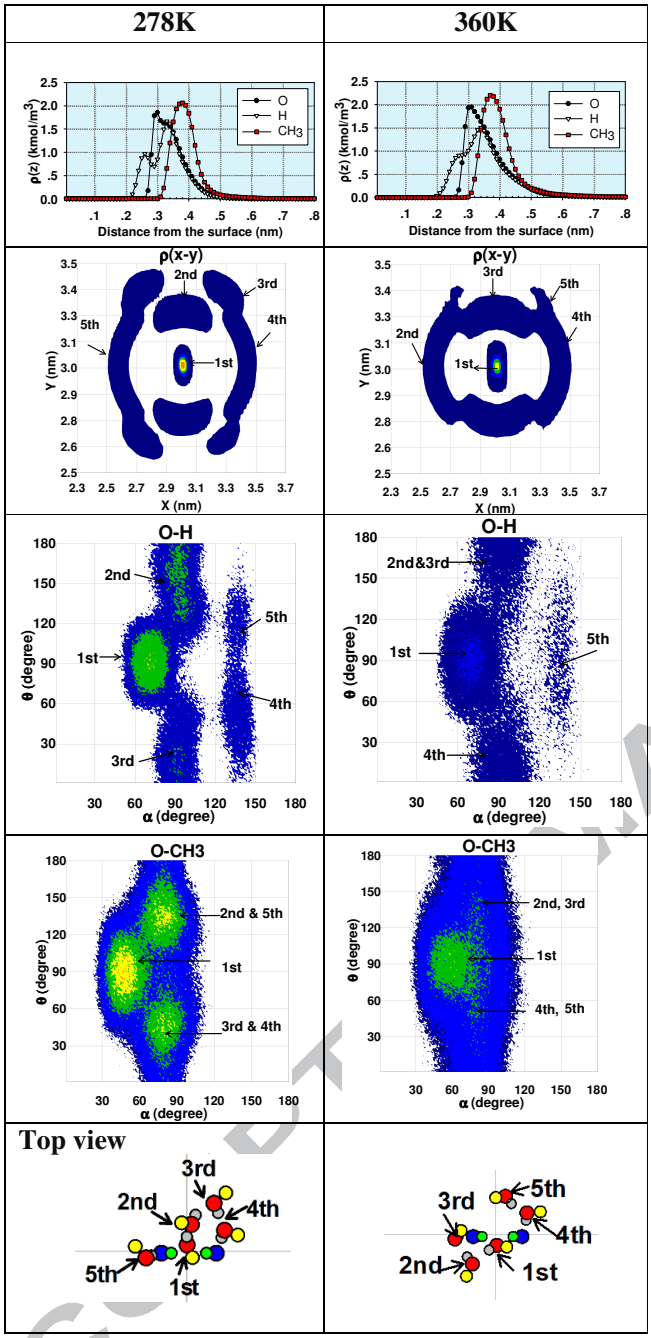

Figure 10. The local density distributions, angular distributions and snapshots at Point IV

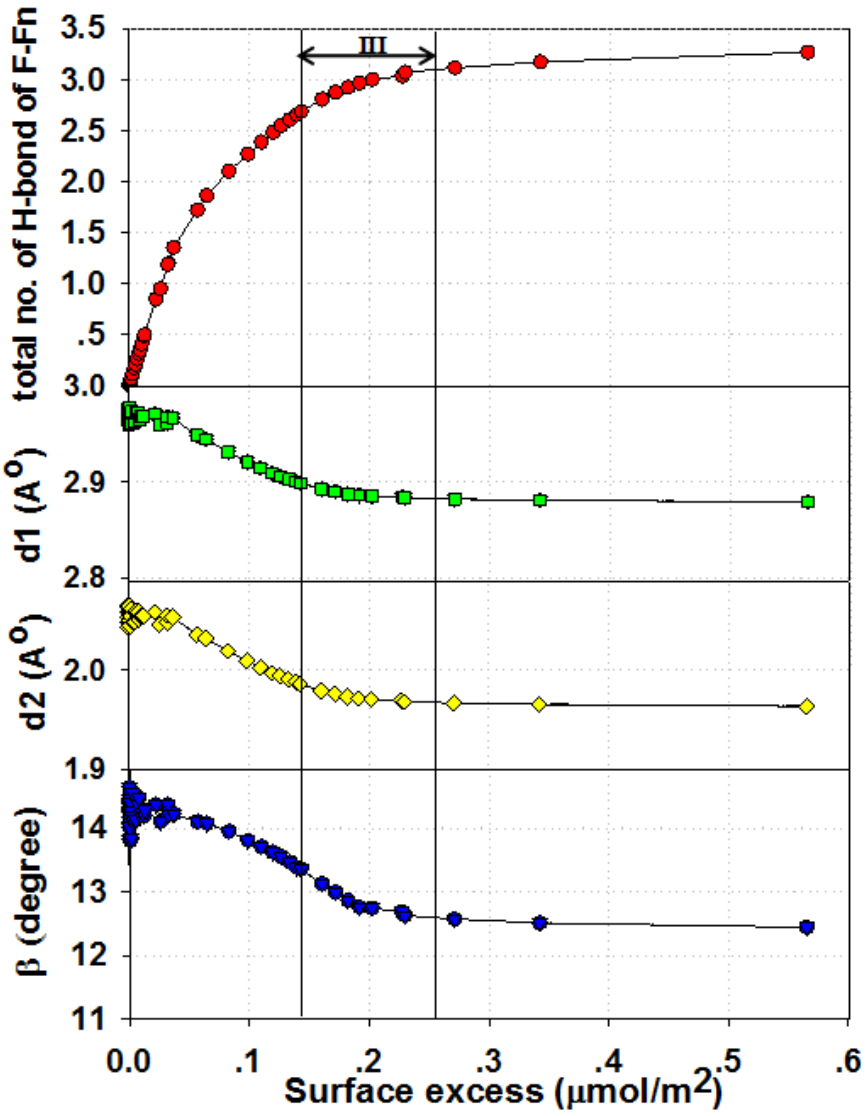

Figure 11. Total number of hydrogen bonds (Top). Averages of the bond lengths d1, d2 and angle beta per hydrogen bond of F-Fn at 278K. The definition of hydrogen bond is shown in Figure 1c.

Region V (278 & 360K): After the functional groups have been saturated at **Point IV**, the isosteric heat increases slightly and then remains constant at 45kJ/mol at 278K. This is due to the increase in the F-F contribution and a modest increase in the F-Gr contribution. On the other hand, the isosteric heat at 360K continues to increase; mostly due to the F-F interactions with a small contribution from the F-Gr interactions. In this region, submonolayer adsorption on the basal plane occurs, initiated by adsorption at the boundary of the methanol cluster at

the functional groups, followed by formation of 2D-molecular clusters in the form of a ring or string as shown in Figure 12. The local density distributions change very slightly with temperature, with some minor population of molecules shifting away from the surface. This shift is greater at higher temperature because of thermal fluctuation. At the end of this section, the basal plane is essentially filled with adsorbate.

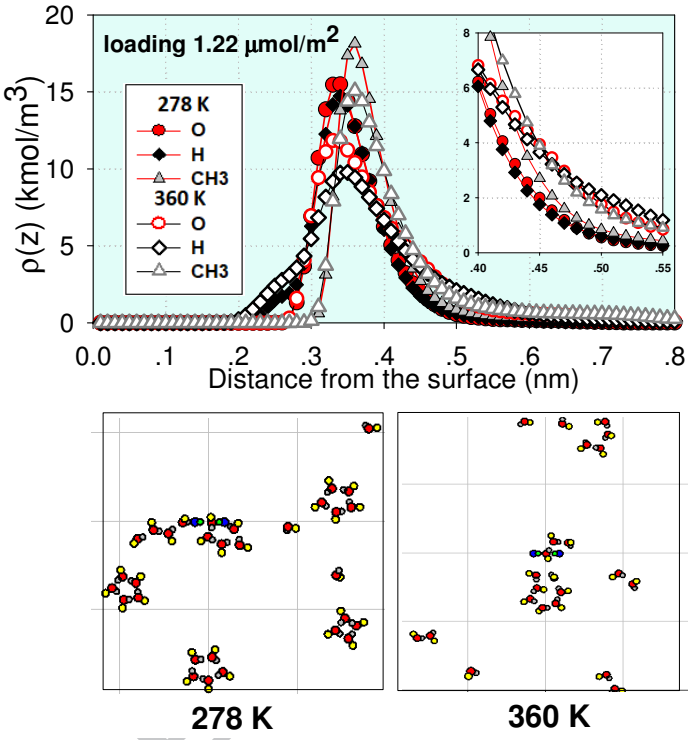

Figure 12. Local density distribution in z direction and snapshots at Region V

Region VI: In this region multilayering occurs as studied in our previous work (Nguyen et al. 2011).

4. Conclusions

We have used GCMC simulation to investigate the behaviour of isosteric heat versus loading for methanol adsorption on two hydroxyl groups attached to a graphite surface, at temperatures ranging from 278K to 360K. We have found that:

(1) The isosteric heat at zero loading is higher than the condensation heat for all temperatures, and decreases with temperature.

(2) When the loading is increased, the isosteric heat decreases, which is associated with the formation of a cluster of molecules around the functional groups. At the incipient saturation of the functional groups there are five adsorbate molecules. Adsorption is initiated on one functional group before extending to the other group. To maximise entropy, the adsorbate molecules are distributed as 4:1 at 278K and 3:2 at 360K, respectively.

(3) The minimum heat is more pronounced with temperature.

Acknowledgement: This work is supported by the Australian Research Council (DP160103540), the Thailand Research Fund (Contract no. TRG5780126) and Thailand National Science and Technology Development Agency (Contract no. TG-33-14-59-062M). The authors acknowledge National e-Science Infrastructure Consortium for providing computing resources that have contributed to the research results reported within this paper.

5. References

Alabadi, A., Razzaque, S., Yang, Y., et al., 2015. Chemical Engineering Journal 281, 606-612.

Allen, M., Tildesley, D., 1989. Computer simulation of liquids. Clarendon Press, Oxford, UK.

Bandosz, T., Jagiełło, J., Schwarz, J., et al., 1996. Langmuir 12(26), 6480-6486.

Chen, B., Potoff, J., Siepmann, J., 2001. The Journal of Physical Chemistry B 105(15), 3093-3104.

Rasmussen, J., Vishnyakov, A., Thommes, M., et al., 2010. Langmuir 26 (12), 10147-10157.

Cychosz, K., Guillet-Nicolas, R., Garcia-Martinez, J., et al., 2017. Chemical Society Reviews 46(2), 389-414.

Nicholson, D., Parsonage, N., 1982. Computer Simulation and the Statistical Mechanics of Adsorption. Acadamic Press, New York, USA.

Do, D., Herrera, L., Do, H., 2008. Journal of Colloid and Interface Science 328(1), 110-119.

Easton, B., Machin, W., 2000. Journal of Colloid and Interface Science 231(1), 204-206

Factorovich, M., Gonzalez, E., Molinero, V., et al. 2014., The Journal of Physical Chemistry C 118(29), 16290-16300.

Fan, C., Do, D., Nicholson, D., 2011. Langmuir 27(7), 3511-3526.

Gregg, S., Sing, K., 1982. Adsorption, Surface Area and Porosity. Academic Press, London, UK.

Joyner, L., Emmett, P., 1948. Journal of the American Chemical Society. 70(7), 2353-2359.

Kaneko, K., 2015. Nature Chemistry 7, 194-196.

Klomkliang, N., Do, D., Nicholson, D., 2014. Langmuir 30(43), 12879-12887.

Klomkliang, N., Do, D., Nicholson, D., 2015.The Journal of Physical Chemistry C 119(17), 9355-9363.

Klomkliang, N., Do, D., Nicholson, D., 2015. AIChE Journal 61(11), 3936-3943.

Klomkliang, N., Kaewmanee, R., Saimoey, S., et al., 2016. Carbon 99, 361-369.

Klomkliang, N., Nantiphar, O., Thakhat, S., et al., 2017. Carbon 118, 709-722.

Kowalczyk, P., Miyawaki, J., Azuma, Y., et al., 2017. Carbon 124, 152-160.

Thommes, M., Bernd, S., Matthijs, G., et al., 2005. Langmuir 22, 756-764.

Miura, K., Morimoto, T., 1991. Langmuir 7(2), 374-379.

Mooney, D., Müller-Plathe, F., Kremer, K., 1998. Chemical Physics Letters 294(1–3), 135-142.

Morimoto, T., Miura, K., 1985. Langmuir 1(6), 658-662.

Morimoto, T., Miura, K., 1986. Langmuir 2(1), 43-46.

Morishige, K., 2006. Langmuir 22, 9220-9224.

Nguyen, V., Phuong, T., Do, D., et al., 2013. The Journal of Physical Chemistry C 117(10), 5475-5484.

Nguyen, V., Do, D., Nicholson, D., 2011. The Journal of Physical Chemistry C 115(32), 16142-16149.

Nguyen, V., Horikawa, T., Do, D., et al., 2013. Carbon 61, 551-557.

Ohba, T., Kaneko, K., 2007. The Journal of Physical Chemistry C 111(17), 6207-6214.

Pagliai, M., 2003., Journal of chemical physics 119(13), 6655-6662.

Pierce, C., Smith, N., 1950. The Journal of Physical and Colloid Chemistry 54(3), 354-364.

Reichenbach, C., Kalies, G., Enke, D., et al., 2011. Langmuir 27(17), 10699-10704.

Roberts, A., Sing, K., Tripathi, V., 1987. Langmuir 3(3), 331-335.

Salame, I., Bagreev, A., Bandosz, T., 1999. Langmuir 15(2), 587-593.

Salame, I., Bandosz, T., 2000. Langmuir 16(12), 5435-5440.

Sarkisov, L., Centineo, A., Brandani, S., 2017. Carbon 118, 127-138.

Sing, K., Everett, H., Haul, W., et al., 1985. Pure and Applied Chemistry 57(4), 603-619.

Steele, A., 1973. Surface Science 36(1), 317-352.

Wongkoblap, A., Do, D., 2007. The Journal of Physical Chemistry B 111(50), 13949-13956.

Yin, F., Mays, T., McEnaney, B., 1999. Langmuir 15(25), 8714-8718.

Zelenka, T., 2016. Microporous and Mesoporous Materials 227, 202-209.

Zeng, Y., Prasetyo, L., Nguyen, V., et al., 2015. Carbon 81, 447-457.

Graphical abstract: